Journal of Photochemistry and Photobiology A: Chemistry 228 (2012) 15–21

Contents lists available at SciVerse ScienceDirect

Journal of Photochemistry and Photobiology A: Chemistry

journal homepage: www.elsevier.com/locate/jphotochem

Preparation of chemically sintered ZnO films and their application in dye sensitized solar cells formed on plastic substrates

P.M. Sirimanne[a,*], H.C. Weerasinghe[b], G.P. Simon[b], Y.B. Cheng[b]

[a] Department of Science and Technology, Uwa Wellassa University, Badulla, Sri Lanka
[b] Department of Materials Engineering, Monash University, Wellington Road, Clayton 3800, Victoria, Australia

ARTICLE INFO

Article history:
Received 5 July 2011
Received in revised form 18 October 2011
Accepted 17 November 2011
Available online 10 December 2011

Keywords:
Polyethelene naphthalate
Polyethyleneimine
Flexible dye sensitized solar cell

ABSTRACT

Meso-porous zinc oxide films were prepared on tin-doped indium oxide-coated, polyethelene naphthalate substrates from binder-free ZnO slurry. The reaction with ammonium hydroxide was found to increase connection between ZnO grains by forming a nano-rod like structure followed by heating at 150 °C. The enhancement of adhesion among ZnO grains was evaluated using a nano-scratch technique. Two different xanthene dyes were used to sensitize ZnO electrodes, with a photo-voltage of 657 mV, fill-factor of 73% and photo-current of 4.1 mA cm^{-2} with a maximum light to-electrical energy conversion efficiency of 2.0% being obtained for the plastic based ZnO|mercurochrome|electrolyte solar cell under 1 sun.

1. Introduction

Dye sensitized solar cells (DSSCs) have been extensively studied due to their potential for manufacturing low cost solar cells compared to that of silicon solar cells [1,2]. In those studies, working electrodes are usually prepared from screen printing semiconductor metal oxide pastes, followed by an annealing at 450–500 °C [1–3]. A sintering process is essential to achieve better electrical contact between the semiconductor and the conducting glass substrate, as well as between metal oxide semiconductor particles. However, employing plastic substrates restricts high temperature sintering processes. Several techniques such as lift-off technique [4], low-temperature heating [5], microwave irradiation [6], hydrothermal crystallization [7] and mechanical compression [8] have been used to fabricate plastic-based dye sensitized solar cells. Improvement of connection among semiconductor metal oxide particles remains a technical challenge in fabrication for DSSCs on plastic substrates, where poor connection between particles leading to lower power conversion efficiencies, compared to that of glass-based cell counterparts. Thus, alternative treatments are required in order to improve the connectivity between inter-particles. In this work a simple technique was investigated to fabricate agglomerate and crack free ZnO films on tin doped indium oxide (ITO) coated polyethelene naphthalate (PEN) substrates (known as ITO|PEN). We have found treatment of ZnO films with ammonium hydroxide increases the connectivity among ZnO grains significantly, by forming a nano-rod like structure. The effect of so-called "chemical" sintering on mechanical and photovoltaic properties of these electrodes is discussed.

2. Experimental

2.1. Preparation of nano-particulate ZnO electrodes

Two grams of ZnO nano-powder (Aldrich) and 5 ml of ethanol were placed in an agate ball milling jar with different size of agate balls. The mixture was then milled at 250 rpm speed for 5 h. ZnO slurry was coated on the conducting side of ITO|PEN substrates (13 Ω cm^{-2}, Peccell Technologies, Inc., Japan) by doctor blade technique. The thickness of ZnO films was maintained as 10 μm. ZnO-coated ITO|PEN substrates were allowed to dry at room temperature for 30 min and were placed horizontally (the film oriented upwards). These electrodes were wetted by aqueous 0.5 M ammonium hydroxide solution and allowed to react with ZnO in atmospheric conditions for 1 h. These electrodes were then placed on a hot plate and the temperature was gradually increased to 150 °C, with a time interval of 30 min with and without UV–ozone post-treatment.

2.2. Mechanical properties of nano-particulate ZnO electrodes

The mechanical properties of nano-porous ZnO electrodes were evaluated from a nano-indenter (Hysitron, U.S.A.). Several well spaced, distinct nano-scratches (14 μm in length and 2 μm in

* Corresponding author. Tel.: +94 (0)55 355 9113.
E-mail address: psirimanne@hotmail.com (P.M. Sirimanne).

1010-6030/$ – see front matter © 2011 Elsevier B.V. All rights reserved.
doi:10.1016/j.jphotochem.2011.11.006

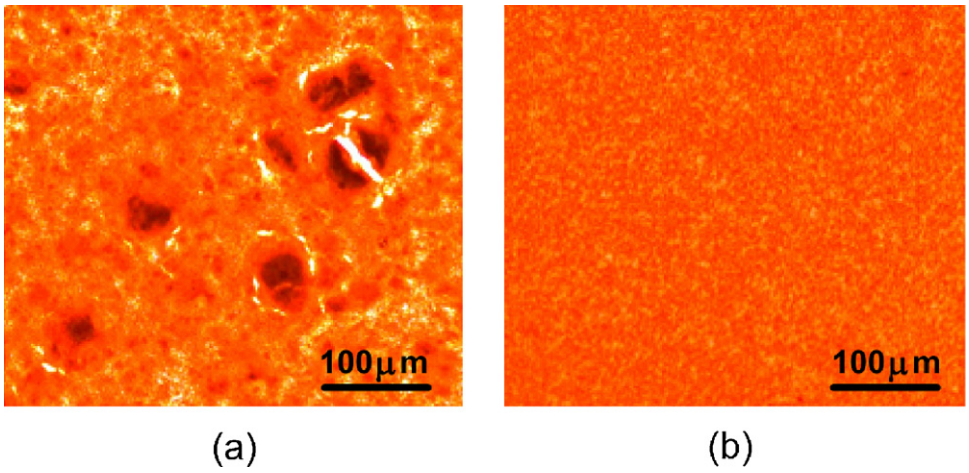

Fig. 1. Optical microscopic images of ZnO films (on ITO|PEN) prepared by using (a) non-milled and (b) milled ZnO slurries.

depth) were produced on the surface of the ZnO electrodes under the displacement control mode. The forces acting on the indenter, in normal and lateral directions are monitored. The amplitude of normal and lateral forces required to produce a scratch of the same size in different ZnO films is an indication of the interparticle connection [9]. The surface morphologies of the ZnO films were analysed using scanning electron microscope (JEOL JSM-840A).

2.3. Preparation of Pt|electrolyte|dye|ZnO cells

ZnO coated ITO|PEN electrodes were sensitized individually by two different dyes mercurochrome (Fluka) and eosin Y (Fluka) by soaking them in relevant dye solutions for one night. Dye coated films were refluxed in ethanol and dried at room temperature, under N_2 atmosphere. Fully plastic dye sensitized solar cells were fabricated by sandwiching a Pt|ITO|PEN films (Peccell Technologies, Japan) with the dye coated ZnO|ITO|PEN electrode using a 25 μm thermoplast hot-melt sealing foil (Solaronix, Switzerland). The electrolyte (a mixture of 0.05 M iodine and 0.50 M tert-propylamonium iodide, in acetonitrile and ethylene-carbanate by volume 4:6) was filled into the space between two electrodes by capillary action. Current–voltage characteristics (*I–V*) and incident photon-to-current-conversion-efficiency (IPCE) of cells with the configuration of Pt|electrolyte|dye|ZnO were studied under irradiation of white light (100 mW cm^{-2}) and monochromatic light using an Oriel solar simulator system. The size of the cell was 0.25 cm^{-2}.

3. Results and discussion

Optical microscopic images of ZnO films prepared using both non-milled [Fig. 1(a)] and milled [Fig. 1(b)] ZnO slurries are shown in Fig. 1. In these images yellow–orange (for interpretation of the references to colour in text, the reader is referred to the web version of the article), dark brown and white colour networks correspond to the ZnO grains, agglomerates and the substrate, respectively. It is also clear that the ZnO films prepared using non-milled ZnO slurries exhibited a high degree of cracking of the films. These cracks are formed due to the high stress around agglomerates created in the drying process. In contrast, the crack and agglomerate free nature can be readily observed on the ZnO films prepared by using milled slurry. In an effort to further link the particles, ammonium hydroxide was used, since it is known that only ZnO dissolves in ammonium hydroxide, whilst the other components in DSSC, In_2O_3, SnO_2 are not soluble at room temperature [10]. Thus dried ZnO|ITO|PEN electrodes were placed horizontally and wetted with an ammonium hydroxide solution at room temperature. The ammonium hydroxide solution lies as a bubble on the ZnO electrode due to surface tension. Dissolution of ZnO forms $Zn(OH)_2$ and then $[Zn(OH)_4]^{2-}$ in the ammonium hydroxide solution. When the temperature of the furnace was increased to 150 °C, water become vaporized and ZnO could be re-formed. Formation of different crystalline phases of ZnO from vaporization of aqueous solution of zinc salts at relatively lower temperature has previously been reported [11]. We also studied the products formed by vaporization of $[Zn(OH)_4]^{2-}$, under different conditions, ZnO was dissolved in an aqueous ammonium hydroxide solution which resulted clear solution which was spread on glass substrates and dried at room temperature and 150 °C, respectively. The resulting white precipitates from the two approaches were removed from the substrates. X-ray diffraction patterns of these products obtained by vaporizing $[Zn(OH)_4]^{2-}$ at (a) room temperature, (b) 150 °C and (c) following UV–ozone at 150 °C and (d) ZnO powder are shown in Fig. 2. No crystalline peak for the white precipitate obtained from vaporizing the $[Zn(OH)_4]^{2-}$ solution at room temperature was observed, indicating the amorphous nature of the product (Fig. 2a). This product did not dissolve in NH_4Cl, and was assumed to be $Zn(OH)_2$ [10]. This amorphous precipitate was then heated to 150 °C and no X-ray diffraction peaks indicating crystallinity were seen for this re-heated sample either, although it dissolved in NH_4Cl. This result

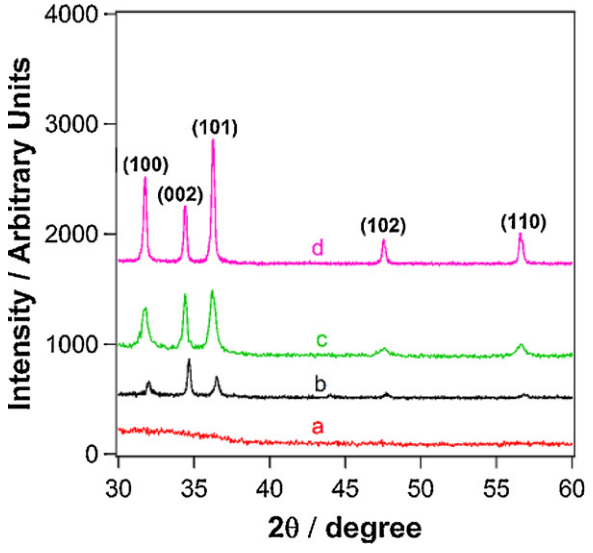

Fig. 2. X-ray diffraction of the product obtained from vaporizing $[Zn(OH)_4]^{2-}$ at (a) room temperature, (b) 150 °C, (d) 150 °C with UV–ozone and (d) ZnO powder.

indicates that $Zn(OH)_2$ was transformed into amorphous ZnO during heat treatment (since ZnO dissolves in NH_4Cl, whilst $Zn(OH)_2$ does not [10]). As is expected, the formation of highly crystalline ZnO was observed for the product obtained by directly vaporizing of $[Zn(OH)_4]^{2-}$ at 150 °C (curve *b*, Fig. 2). A relative enhancement of the intensity of (0 0 2) crystalline plane and a slight shift of all peaks toward the higher angles were observed for this sample compared to that of powder sample. Growth of specifically oriented crystallographic planes is a peculiar property of thin films and the observed shift may be due to impurities, oxygen defects or/and contraction of adjacent layers (caused by tensile stress) in the film, compared to that of polycrystalline powder sample [12]. Such a shift was not observed for the sample obtained by vaporizing of $[Zn(OH)_4]^{2-}$ at 150 °C in the presence of UV–ozone (curve *c*, Fig. 2), showed the predominant orientation of (1 0 1) crystalline plane. These results clearly indicate formation of different types of ZnO, depending on the experimental conditions applied for vaporizing of $[Zn(OH)_4]^{2-}$. However, we are not in a position to give exact reason why no shift in the XRD pattern under UV–ozone treatment e compared to that of the powder sample, at the present stage of research.

The morphology of these films was studied using scanning electron microscope (SEM) and images of ZnO films (a) before and (b) after ammonium hydroxide treatment are shown in Fig. 3. An interconnected net-work of ZnO grains was observed for the film prepared by doctor blade technique (Fig. 3a). In addition to this interconnecting network, formation of a nanorod-like structure was observed on the surface of the ZnO films after ammonium hydroxide treatment (Fig. 3b). Even thought formation of nanorods-structure is ambiguous they act as an additional adhesive mechanism, improving connectivity between the ZnO grains. The improvement of mechanical strength of ZnO films due to such a "necking" morphology being formed was also systematically evaluated using a nano-indentation technique we developed [9]. The force curves for normal (A) and lateral (B) forces for indentation measurements on the ZnO electrodes prepared on the ITO|PEN substrates are shown in Fig. 4, without any ammonium hydroxide treatment (curve *a*), and following ammonium hydroxide treatment (curve *b*). The enhancement in both normal and lateral forces gives evidence of improving of adhesion between ZnO particles, by the ammonium hydroxide treatment. A further test (and very important in a practical, end-use sense) of the mechanical integrity of treated ZnO film was evaluated by continuous bending. These films exhibited a high degree of stability over 250 times continuous bending ($30° < \theta < 90°$). A photographical image of the ZnO film after 250 times of continuous bending is shown in Fig. 5.

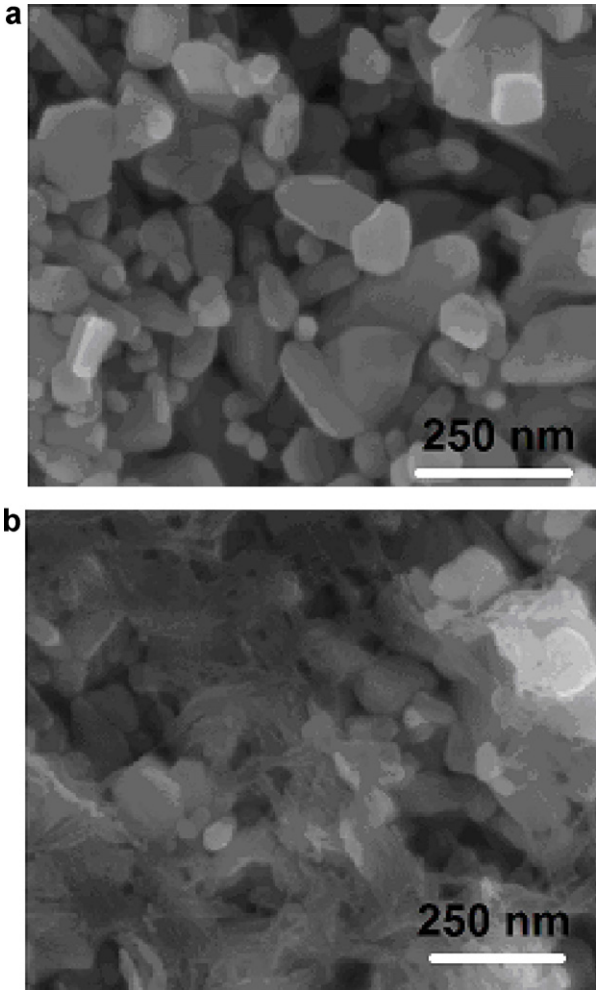

Fig. 3. Scanning electron microscopic images of the surface of ZnO films (a) before and (b) after ammonium hydroxide treatment.

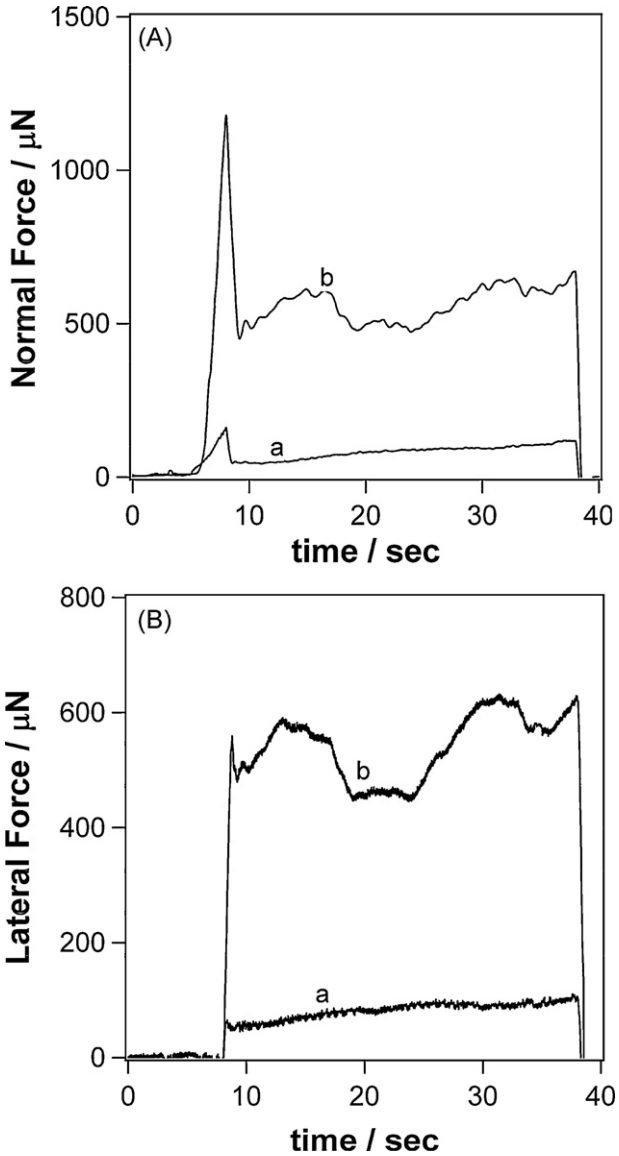

Fig. 4. The variation of (A) normal and (B) lateral forces for ZnO electrodes prepared on ITO|PEN substrates (a) untreated and (b) treated with ammonium hydroxide.

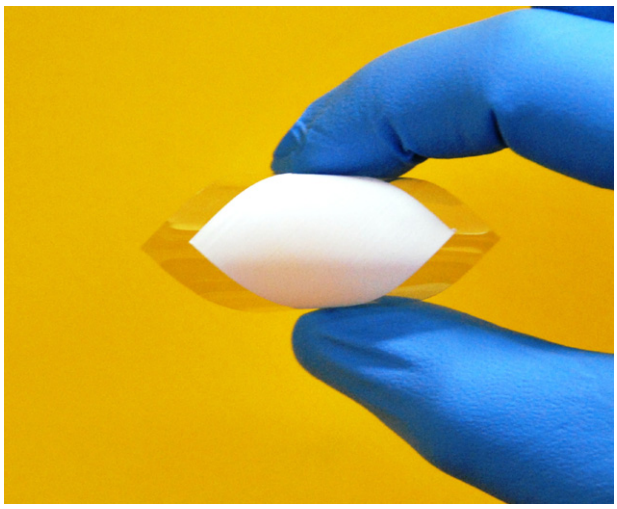

Fig. 5. Image of ZnO film after 250 times continuous bending.

The ZnO films prepared were sensitized by two different xanthene dyes, The chemical structures of dyes (a) eosin Y and (b) mercurochrome are shown in Scheme 1. Significant differences exist between two dye molecules. A mercury atom with a hydroxyl group in the mercurochrome molecule has replaced from Br molecule in eosin Y molecule. Firstly, the solubility of these dyes in different solvents was studied. Eosin Y easily dissolved in water, ethanol, acetonitrile, whilst mercurochrome dissolves water and ethanol but not in acetonitrile. However, both dyes do not dissolve in even basic aromatic solvents such as benzene. Absorption spectra of eosin Y and mercurochrome exhibited peculiar properties at 10^{-3} M due to the self aggregation of dye molecules Fig. 6(A). No significant change in the shape of absorption spectrum was observed due to change of solvent at higher concentrations of dye. Absorption spectra for eosin Y in (a) water, (b) ethanol and (c) acetonitrile at 10^{-5} M are shown in Fig. 6(B). Eosin Y exhibits two well-separated absorption bands in dilute dye solutions ($\sim 10^{-5}$ M). In addition, a slight shift was observed in the absorption spectra due to change in the solvent, and is a well-known known effect [13]. The observed absorption hump and the maxima in Fig. 6(B) correspond to (1, 0) and (0, 0) vibronic bands of eosin Y monomers [14,15]. Further, we have diluted dye solutions of higher concentrations by the mixtures of used solvents. Such diluted dye solutions also exhibited similar type of vibronic exciton bands. However, the wavelength correspond to the maximum absorption was shifted with the ratio of the solvents. Absorption spectra for mercurochrome in (a) water and (b) ethanol with the same concentration are also shown in Fig. 6(C). Mercurochrome also exhibited similar behaviour to that of eosin Y. Diffuse-reflectance spectra of eosin Y coated ZnO electrodes prepared by using different dye solutions (a) water, (b) ethanol and (c) acetonitrile are shown respectively in Fig. 7(A). As can be seen,

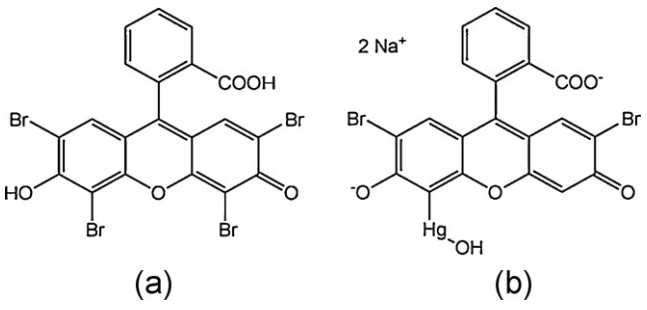

Scheme 1. Chemical structure of (a) eosin Y and (b) mercurochrome.

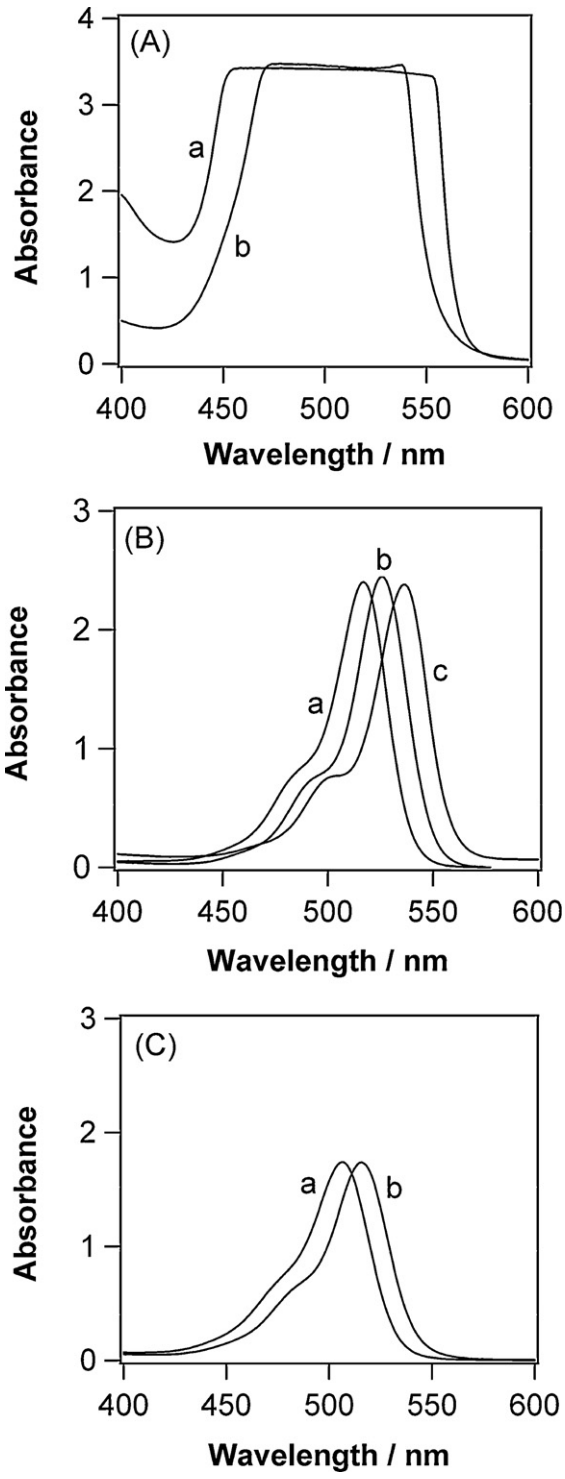

Fig. 6. (A) absorption spectra of (a) eosin Y, (b) mercurochrome at concentration of 10^{-3} M, (B) absorption spectra of eosin Y (a) water, (b) ethanol, (c) acetonitrile at concentration of 10^{-5} M, and (C) absorption spectra of mercurochrome (a) water, (b) ethanol at concentration of 10^{-5} M.

no significant shift in the peak positions was observed in the diffuse reflectance spectra of sensitized ZnO films prepared by the same dye in different solvents. This result indicates that a similar type of chemical bond was formed between dye molecules and ZnO films, even though the dye itself behaves differently in various solvents. In addition, no significant shift was observed in the diffuse reflectance spectra of sensitized ZnO films with the change of the amount of loaded dye on the electrode. Diffuse-reflectance spectra

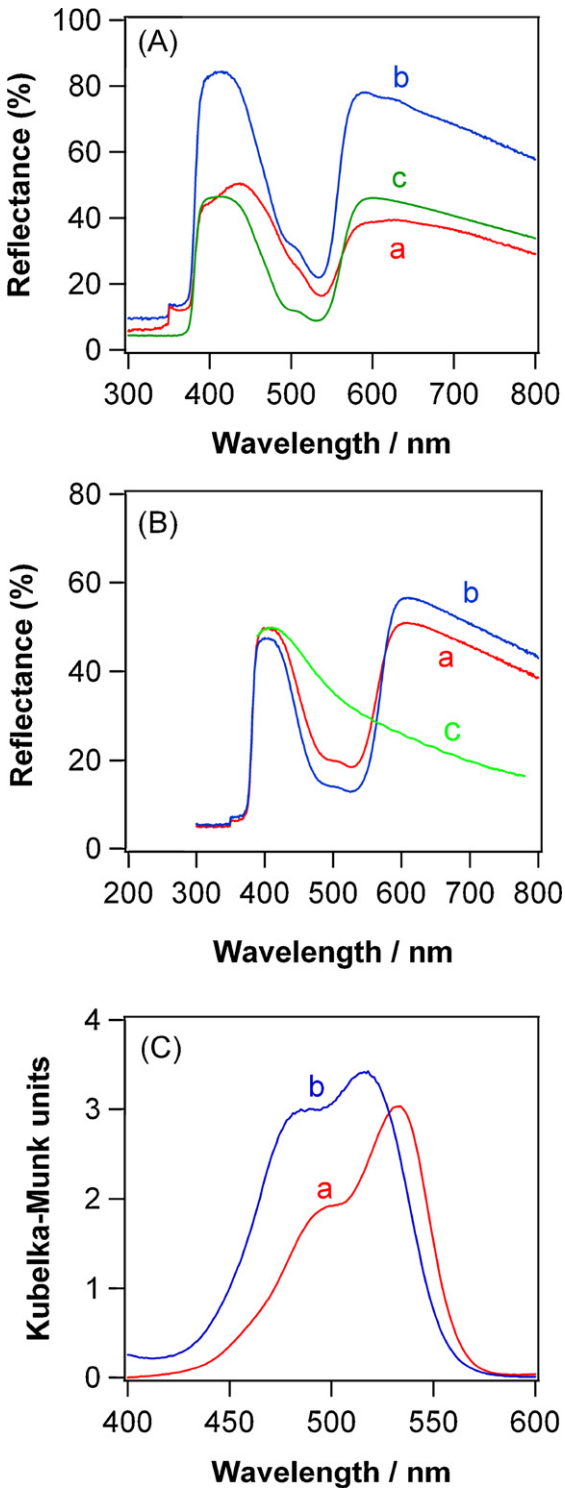

Fig. 7. (A) Diffuse reflectance spectra of eosin Y coated ZnO electrodes prepared by immersing in different dye solutions (a) water, (b) ethanol (c) acetonitrile, (B) diffuse reflectance spectra of mercurochrome coated ZnO electrodes prepared by immersing in different dye solutions (a) water, (b) ethanol and (c) diffuse reflectance spectra of ZnO and (C) absorption spectra (in Kubelka–Munk units) of dye coated ZnO electrode for (a) eosin Y and (b) mercurochrome.

of mercurochrome coated ZnO electrodes prepared by using different dye solutions (a) water and (b) ethanol are also shown in same figure (Fig. 7B). These spectra were converted to corresponding absorption spectra by applying the Kubelka–Munk equation, and the absorption spectra of the sensitized ZnO films for (a) eosin Y and (b) mercurochrome, at the optimum dye absorption condition, are shown in Fig. 7(C). These two spectra are in contrast to absorption spectra for dye solutions shown in Fig. 6(B) and (C), where broadening of the spectrum after attaching dye molecules on to ZnO and shift of spectra toward the longer wavelengths is seen. As is observed, significant enhancement in the (1, 0) vibronic band was observed compared to the (0, 0) vibronic band after bonding dyes with ZnO, compared to what is seen in dye solutions [from the comparison of graphs Figs. 7(C) and 6(B) or (C)]. The absorption spectrum of eosin Y sensitized ZnO films [curve *a* in Fig. 7(C)] match well the dimmer spectra of eosin Y, as reported previously [14]. Mercurochrome also behaves in a similar manner when in contact with ZnO, and these results clearly indicate eosin Y and mercurochrome exist as aggregates in solutions of higher dye concentration, as monomers in diluted solutions, and dimmer on ZnO electrodes.

The excited levels of both dyes lie energetically at a level greater than the conduction band of ZnO. Thus injection of electrons form excited state of dye molecules to the conduction band of ZnO is thermodynamically favourable process [3,16]. Photovoltaic characteristics of electrolyte|dye|ZnO cells prepared are shown for those (a) treated with ammonium hydroxide and (b) non-treated ZnO

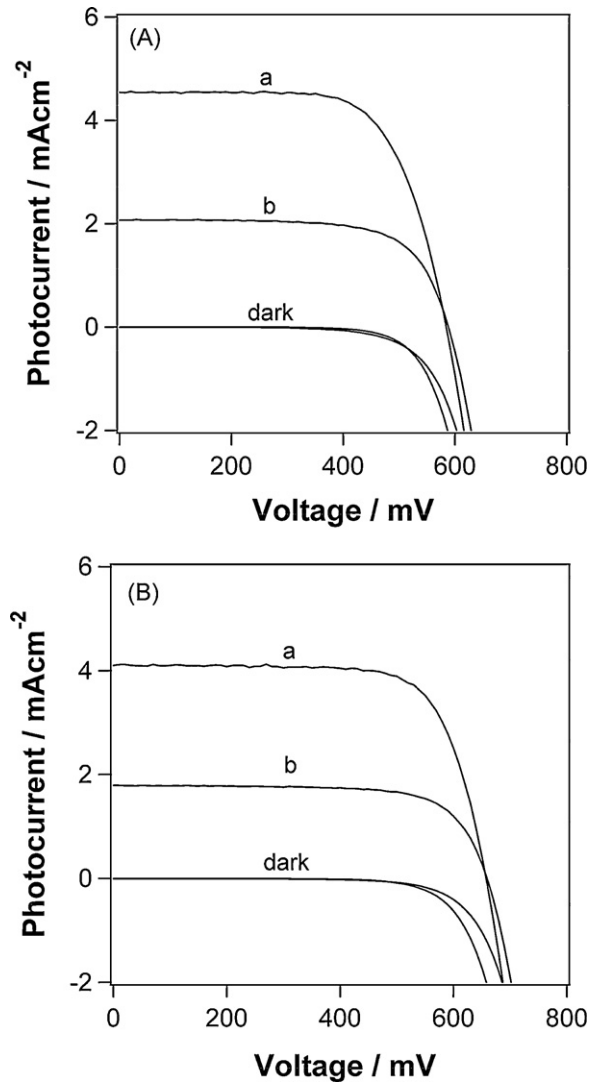

Fig. 8. Current–voltage characteristics of electrolyte|dye|ZnO cell for (A) eosin Y and (B) mercurochrome prepared by using (a) treated with ammonium hydroxide and (b) non-treated ZnO films. Effective area of the cell is 0.25 cm^2.

Table 1
The performances of electrolyte|dye|ZnO cells for different configurations, where ele., MC, EY denote electrolyte, mercurochrome and eosin Y.

Cell configuration	V_{OC} (mV)	I_{SC} (mA cm^{-2})	ff (%)	η (%)	IPCE (%)	R_0 (Ω)	R_1 (Ω)	R_2 (Ω)
Pt|ele|MC|ZnO|ITO	659	1.79	72	0.85	41	20.97	3.1	5.2
Pt|ele|MC|$ZnO_{treatred}$|ITO	657	4.1	73	8	54	19.58	2	3.6
Pt|ele|EY|ZnO|ITO	588	2.07	70	0.85	47	24.63	1.8	3.81
Pt|ele|EY|$ZnO_{treatred}$|ITO	584	4.54	69	1.82	59	22.96	1.79	3.1

films for (A) eosin Y and (B) mercurochrome are shown in Fig. 8. The photo-voltaic performance of ZnO|dye|electrolyte cells with different configurations on plastic substrates are shown in Table 1. A clear enhancement in short-circuit photocurrent and efficiency are observed after ammonium hydroxide treatment on ZnO films compared to that of cells with non-treated ZnO films. No significant variation was observed in voltage and fill-factor after ammonium hydroxide treatment. The maximum open circuit voltage (V_{OC}) of 657 mV, a fill-factor (ff) of 73%, a reasonably higher short-circuit photocurrent (I_{SC}) of 4.10 mA cm^{-2} and efficiency (η) of 2.0% were observed for the plastic based ZnO|mecurochrome|electrolyte cell prepared by using ammonium hydroxide treatment. We have compared our results with previously reported cell parameters for plastic based ZnO|dye|electrolyte cells. The Maximum photo-performances were observed for plastic based ZnO cells sensitized using a styryl dye [17]. In that study, the maximum I_{SC} of 6.22 mA cm^{-2}, V_{OC} of 0.53 V, ff of 0.59 and η of 1.94 were observed under 1 sun illumination. Wei et al. has also studied photo-properties of plastic based solar cells with a configuration of ZnO|black dye|electrolyte [18], and a maximum I_{SC} of 2.33 mA cm^{-2} and V_{OC} of 0.23 V were observed under 1 sun illumination. Our observed V_{OC} of 657 mV and fill-factor (ff) of 73% are higher than the values obtained in those cases, and may indicating a particularly strong bonding between ZnO and either the mercurochrome or eosin Y molecules. ZnO|mercurochrome|electrolyte cells were found to exhibit a much higher photovoltage and efficiency compared to ZnO|eosin Y|electrolyte cell under similar conditions. The dye mercurochrome has relatively greater number of hydroxyl groups compared to eosin Y, thus possessing a greater capability of strong bonding with ZnO, and is likely the reason for enhancement of photo-performance in ZnO|mercurochrome|electrolyte cells. An attempt has been made to evaluate the amount of dye absorbed onto the electrodes by soaking them individually in solvents such as KOH, CH_3COOH, HCl, HNO_3, C_2H_5OH and CH_3OH. Neither dye molecules were able to be dissolved into the alcohols, although rapid desorption of dye molecules was observed into acidic and basic solutions due to dissolution of ZnO in these acids and bases. The dye concentration of sensitized ZnO electrodes for mercurochrome and eosin Y was evaluated to be $\sim 10^{17}$ molecules/cm^2 for both systems, at the optimum photocurrent generation, determined by soaking them in a KOH solution of pH 10.5. The IPCE spectra for electrolyte|eosin Y|ZnO cells prepared using (a) treated and (b) non-treated films are shown in Fig. 9. The maximum IPCE of 59% was observed for ZnO|eosin Y|electrolyte cells prepared by using treated ZnO film. Observation of similar properties in action spectra to that of diffused reflectance spectra indicates charge generation by dimmers. Charge generation in the ZnO|dye|electrolyte cell can be summarized as follows,

At photo-anode

$$D_2 + h\nu \rightarrow D_2^* \rightarrow e^-_{CB_{ZnO}} + D_2^+ \quad \text{(i)}$$

$$2D_2^+ + 3I^- \rightarrow I_3^- + 2D_2$$

At the dark-cathode

$$I_3^- + 3e \rightarrow 3I^- \quad \text{(ii)}$$

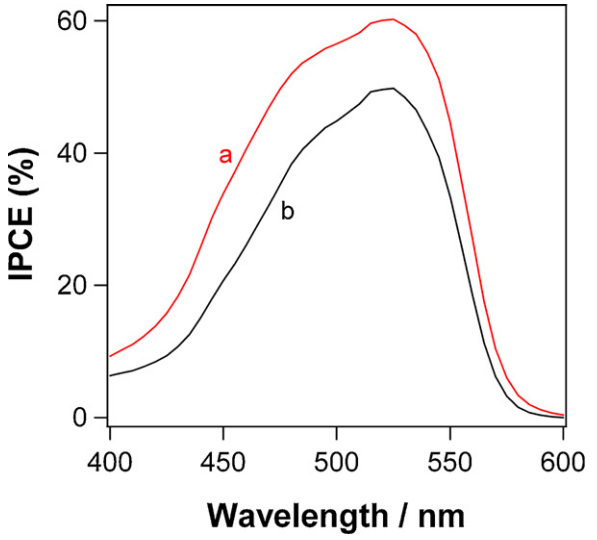

Fig. 9. Incident photon-to-current conversion efficiency of electrolyte|eosin Y|ZnO cell for (a) treated with ammonium hydroxide and (b) non-treated ZnO films.

where D_2 is the dimmer of eosin Y or mercurochrome molecule, D_2^* is the excited dye molecule and CB_{ZnO} is the conduction band of the ZnO. Electrical impedance spectroscopy was carried out to examine the interfacial electrical properties of dye sensitized devices. Impedance spectra for the electrodes prepared using eosin Y for (a) non-treated and (b) treated with ammonium hydroxide are shown in Fig. 10. Two typical semicircles in Nyquist plots corresponding to high range of frequencies (left semicircle with radius of R_1) and middle range of frequencies (right semicircle with radius of R_2) are observed. The intercept of the graph at higher frequency range (R_0) corresponds to the ohmic resistance of the cell (i.e.; resistance of the base ITO layer of the TiO_2 electrode). R_1 corresponds to the charge transfer at counter electrode (reduction of I_3^- at Pt electrode) and/or electrical contact between the ITO|TiO_2 or TiO_2 particles, whilst R_2 corresponds to the charge transfer process at TiO_2|dye|electrolyte interface [19]. The Nyquist plots were found to shift in the direction of lower impedance after ammonia treatment due to the formation of strong bonds between ZnO film and

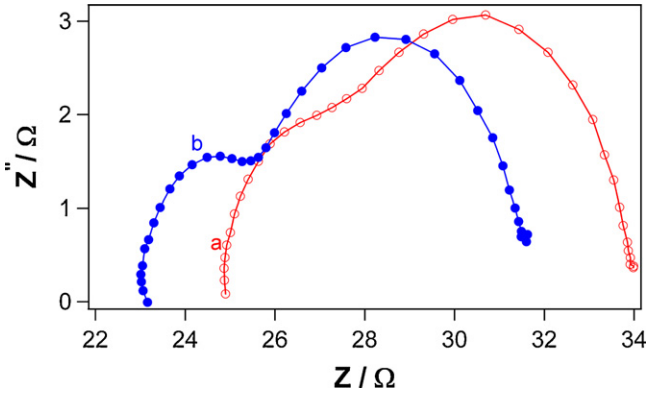

Fig. 10. Impedance spectra of electrolyte|eosin Y|ZnO cells prepared using (a) non-treated and (b) treated with ammonium hydroxide ZnO films.

the substrate. In addition the significant decrease in R_2 provides further evidence for the improved particle–particle, as well as the film–substrate, connectivity.

4. Conclusion

Binder-free ZnO paste was used to fabricate thin films of ZnO on ITO|PEN substrates. It was found that connectivity between the ZnO grains was able to be improved by treatment with ammonia reaction, without the need for high temperature annealing. Two different xanthene dyes were used to sensitize ZnO films for photovoltaic studies. These dyes were found to behave as aggregates in solutions for higher concentration ($>10^{-3}$ M), as monomers in dilute solutions (10^{-5}–10^{-6} M) and as dimmers on ZnO electrodes. The highest photo-voltage of 657 mV, photo-current of 4.1 mA cm^{-2}, fill-factor of 73% with the maximum light to-electrical energy conversion efficiency of 2.0% were obtained for plastic based ZnO|Mercurochrome|electrolyte solar cell under 100 mW cm^{-2} illuminations.

Acknowledgements

Financial support by the Victorian Consortium in Organic Solar Cells (VICOSC) and research facilities provided by the ARC Centre of Excellence for Electromaterials Science and the Royal Melbourne Institute of Technology University are appreciated by the authors.

References

[1] B. O'Regan, M. Graetzel, Nature 353 (1991) 737.
[2] S. Ito, T.N. Murakami, P. Comte, P. Liska, C. Graetzel, M.K. Nazeeruddin, M. Graetzel, Thin Solid Films 516 (2008) 4613.
[3] K. Hara, T. Horiguchi, T. Kinoshita, K. Sayama, H. Arakawa, Solar Energy Mater. Solar Cells 90 (2006) 151.
[4] M. Durr, A. Schmid, M. Obermaier, S. Rosselli, A. Yasuda, G. Nelles, Nat. Mater. 4 (2005) 607.
[5] T.N. Murakami, Y. Kijitori, N. Kawashima, T. Miyasaka, J. Photochem. Photobiol. A: Chem. 164 (2004) 187.
[6] S. Uchida, M. Tomiha, H. Takizawa, Electrochem. Soc. Inc. 206 (2004), A_2.
[7] D. Zhang, T. Yoshida, K. Furuta, H. Minoura, J. Photochem. Photobio. A: Chem. 164 (2004) 159.
[8] T. Yamaguchi, N. Tobe, D. Matsumoto, H. Arakawa, ChemComm (2007) 4767.
[9] H.C. Weerasinghe, P.M. Sirimanne, G.P. Simon, Y.B. Cheng, J. Photochem. Photobiol. 206 (2009) 64.
[10] D.R. Lide, CRC Handbook of Chemistry and Physics, CRC Press, 2008–2009.
[11] A.S. Shaporev, V.K. Ivanov, A.E. Baranchikov, O.S. Polezhaeva, Y.D. Tret'yakov, Russ. J. Inorg. Chem. 52 (2007) 1811.
[12] J. Hinze, K. Ellmer, J. Appl. Phys. 88 (2000) 2443.
[13] P.M. Sirimanne, Renew. Energy 33 (2008) 1424.
[14] D. Fornasiero, T. Kurucsev, J. Chem. Soc., Faraday Trans. 2 (82) (1986) 15.
[15] G.R. Jones, D.A. Duddell, D. Murray, R.B. Cundall, R. Catterall, J. Chem. Soc., Faraday Trans. 2 (80) (1984) 1201.
[16] W.J. Lee, A. Suzuki, K. Immaeda, H. Okada, A. Wakahara, A. Yoshida, J. Appl. Phys. 43 (1) (2004) 152.
[17] T. Dentani, K. Nagasaka, K. Funabashi, J. Jin, T. Yoshida, H. Minoura, M. Matsui, Dyes Pigments 77 (2008) 59.
[18] D. Wei, H.E. Unalan, D. Han, Q. Zhang, Q.L. Niu, G. Amaratunga, T. Ryhanen, Nanotechnology 19 (2008) 424006.
[19] D. Kuang, C. Klein, Z. Zhang, S. Ito, J.E. Moser, S.M. Zakeeruddin, M. Graetzel, Small 3 (12) (2007) 2094.